

Vacancy induced zero energy modes in graphene stacks: The case of ABC trilayer

Eduardo V. Castro^a, M. Pilar López-Sancho^b, María A. H. Vozmediano^b

^aCFIF, Instituto Superior Técnico, TU Lisbon, Av. Rovisco Pais, 1049-001 Lisboa, Portugal

^bInstituto de Ciencia de Materiales de Madrid, Consejo Superior de Investigaciones Científicas, Cantoblanco, 28049 Madrid, Spain

Abstract

The zero energy modes induced by vacancies in ABC stacked trilayer graphene are investigated. Depending on the position of the vacancy, a new zero energy solution is realised, different from those obtained in multilayer compounds with Bernal stacking. The electronic modification induced in the sample by the new vacancy states is characterised by computing the local density of states and their localisation properties are studied by the inverse participation ratio. We also analyse the situation in the presence of a gap in the spectrum due to a perpendicular electric field.

Keywords: Electronic properties, Multilayer graphene, Zero-energy modes.

1. Introduction

Recent experimental advances aiming to generate better samples for electronic devices have allowed the obtention of high quality samples not only of monolayer graphene but also of bilayer graphene (BLG) and trilayer graphene (TLG) [1, 2, 3]. One of the major problems preventing applications of monolayer graphene is the difficulty to open and control a gap in the samples. To this respect bilayer and multilayer samples are more promising [1]. The band structure of few layer graphenes depends on the stacking order [4, 5, 6], what offers the possibility of tuning electronic properties. After the great excitement awakened by the bilayer compound due to the possibility of opening a tunable gap with an external gate [7, 8, 1] the interest has moved recently to the trilayer materials due to their enigmatic properties. As in the Bernal AB stacked BLG an external electric field allows a tunable band gap in the ABC-stacked TLG [9, 10, 11] while the ABA-stacked TLGs are semimetals with electric field tunable band overlap [2, 12].

Structural defects – vacancies, ad-atoms, and other – which may appear during the fabrication process are very important in the graphene materials. While in the first times after the synthesis the concern was that they may deteriorate the performance of graphene-based devices, later tendencies point to their positive use in some applications, as they make it possible to tailor the local properties of graphene and to achieve new functionalities [13]. Being one-atom thick the graphene materials are extremely sensitive to the presence of adsorbed atoms and molecules and, more generally, to defects such as vacancies, holes and/or substitutional dopants. This property, apart from being directly usable in molecular sensor devices, can also be employed to tune graphene electronic properties. The possibility of a controlled manipulation of atoms and molecules on graphene has opened a new area of research that allows to observe chemical interactions or structural modifications of low contrast molecules or nano-objects [14]. Among the defect-induced properties in graphene, magnetism is one of the most

appealing [15, 16, 17, 18]. Recent experimental findings [19] have ascertain the role of vacancies in the magnetic properties of the material.

Vacancies are recognised as important scattering centers in monolayer and BLG [20] and are known to induce zero-energy modes [21] that modify the low-energy properties of the samples. The existence and nature of localised states arising from vacancies in BLG was analyzed in a recent paper [22]. It was found that the two different types of vacancies that can be present in the bilayer system give rise to two different types of states: quasilocalised states, decaying as $1/r$ at long distances r from the vacancy, similar to these found in the monolayer case [23], and truly delocalised states whose wave function remains constant as $r \rightarrow \infty$. These later new midgap states were found to become localised inside the gap induced in the bilayer sample by the electric field effect. The analysis of these vacancy-induced states was generalized in [22] to multilayer graphene systems with ABAB... Bernal stacking. The recent experimental and theoretical activity around the trilayer compounds [24, 5, 25, 26, 27] has shown that the system in the rhombohedral ABC stacking has very different electronic properties than its Bernal partner.

In this paper we will revise the situation of the midgap states induced by vacancies in few layers graphene, with especial attention to TLG. We will see that the ABC-rhombohedral stacked presents yet a new type of zero-energy state with no analogue in the mono or bilayer compounds. The characterisation of this new state exhausts the possibilities for the vacancy states in multilayer graphene with the usual stacking. The paper is organized as follows: in section 2 we give a summary of the situation encountered in the bilayer system and its extension to multilayer graphene with Bernal (AB) stacking. Next we explain in section 3 the new aspects encountered in the trilayer material with rhombohedral (ABC) stacking. In section 4 we summarise the analysis of the work and discuss possible physical consequences.

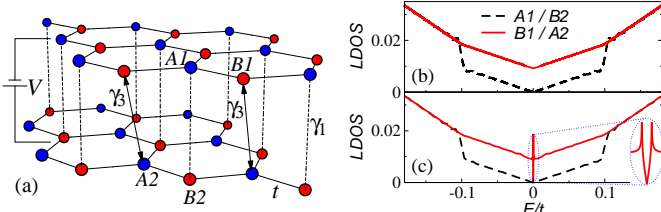


Figure 1: (color online). (a) Bilayer lattice structure and main tight-binding parameters. (b) The general shape of the density of states for the minimal model. The inset shows the changes in the DOS near the Fermi point when the various tight binding parameters are included.

2. Vacancy states in Bernal stacked multilayer graphene

The study and characterisation of vacancy states in monolayer graphene has been an important subject that started prior to the synthesis of the material and continues to our days [15, 19] driven in part by the search for magnetism in *sp* carbon compounds [16]. In the monolayer case there is only one type of vacancy whose presence induces two degenerate quasi-localised states at the Fermi energy. An analytic construction of the wave function of the vacancy was done in [23] by matching surface state solutions at zigzag edges with those localised at Klein edges for a suitable boundary condition. In the continuum limit the wave function can be written as

$$\Psi(x, y) \approx \frac{e^{i\mathbf{K}\cdot\mathbf{r}}}{x + iy} + \frac{e^{i\mathbf{K}'\cdot\mathbf{r}}}{x - iy}, \quad (1)$$

where \mathbf{K} and \mathbf{K}' are the reciprocal space vectors of the two inequivalent corners of the first Brillouin zone, and (x, y) are distances in a reference frame centred at the vacancy position. The wave function is peaked at the position of the vacancy and decays as $1/r$ away from it, a behaviour termed quasi-localised.

This procedure to describe vacancy states was generalised to the AB stacked BLG in [22]. Because of the similitudes with the trilayer case and to fix the notation we will present the main features of the bilayer in some detail in what follows.

The lattice structure of a BLG is shown in Fig. 1. In the AB-Bernal stacking the top layer is shifted with respect to the bottom layer by one C-C distance. As a result only half of the atoms in any layer have a direct neighbour joined by γ_1 in the other layer. We use indices 1 and 2 to label the top and bottom layer, respectively. The main tight-binding hopping parameters are also shown in the figure as well as the different electronic structure near the Fermi level for different values of the tight binding parameters. In the minimal model adopted in most of the works only γ_1 is different from zero [7]. The estimated values of the parameters are $t \sim 3eV$ and $\gamma_1/t \sim 0.1$ [15].

In the Bernal BLG there are two different types of vacancies giving rise to unpaired atoms: vacancies located at A1/B2 or B1/A2 [see Fig. 1(a)]. The first type A1/B2 is produced by removing a site having a neighbour in the adjacent layer and is usually named β vacancy. The second type B1/A2 resulting when the removed site is not connected to the other layer is called α .

We obtained an analytical solution for the states induced by these two types of vacancies in [22] generalising the procedure

done in the monolayer case [23]. For vacancies at A1/B2 sites the wave function obtained is the same given by Eq. (1) which corresponds to a quasi-localised, zero-energy state decaying as $1/r$ around the vacancy in the same layer where the vacancy sits but in the opposite sublattice. This vacancy has then the same properties as these found in the monolayer case. The new state found in [22] corresponds to vacancies at B1/A2 lattice sites. The solution in this case has the form

$$\Upsilon(x, y) \sim \left[\Psi(x, y), \frac{\gamma_1}{t} \frac{x - iy}{x + iy} e^{i\mathbf{K}\cdot\mathbf{r}} + \frac{\gamma_1}{t} \frac{x + iy}{x - iy} e^{i\mathbf{K}'\cdot\mathbf{r}} \right], \quad (2)$$

where $\Psi(x, y)$ is the quasi-localised state given in Eq. (1), and the two component wave function $\Upsilon \sim [\phi_1, \phi_2]$ refers to the two layers; first and second components for the first and second layers, respectively. This is a delocalised state, with the peculiarity of being quasi-localised in one layer (where the vacancy sits) and delocalised in the other where it goes to a constant when $r \rightarrow \infty$.

The same analytical construction followed for the minimal model in BLG can be directly applied to multilayer graphene in Bernal stacking and for the particular case of the ABA TLG. The quasi-localised state (1) is a solution in any multilayer with a A1/B2-vacancy. For a B1/A2-vacancy the solution is a generalisation of state (2) with a quasi-localised component in the layer where the vacancy resides and delocalised components in the layers right on top and below this one: $\Phi(x, y) \sim [\Psi(x, y), \Upsilon_2(x, y), \Upsilon_2(x, y)]$, where $\Upsilon_2(x, y)$ refers to the second component in the right hand side of Eq. (2).

The behaviour of the vacancy states was ascertained in the bilayer system by numerical calculations. A summary of the findings of our previous work on Bernal stacked multilayer graphene is the following: Associated to the presence of vacancies and to the existence of a gap in the spectrum generated by an electric field E_z three different types of behaviour for vacancy-induced states are found:

1. For $E_z = 0$ a β -vacancy (A1/B2 site) induces quasi-localized state ($1/r$ behaviour).
2. For $E_z = 0$ an α -vacancy (B1/A2 site) induces a resonance due to a delocalized state.
3. For $E_z \neq 0$ a β -vacancy produces a resonance inside the continuum near the band edge while an α -vacancy gives rise to a truly localized state inside the gap. This is the most interesting state for the magnetic implications.

3. ABC trilayer

3.1. Model

We follow the tight-binding approximation and consider the minimal model where the in-plane hopping energy, t , and the inter-layer hopping energy, γ_1 , define the most relevant energy scales. This is the minimal model for AB stacked multilayer graphene described above. The simplest tight-binding Hamiltonian describing non-interacting π -electrons in TLG then reads:

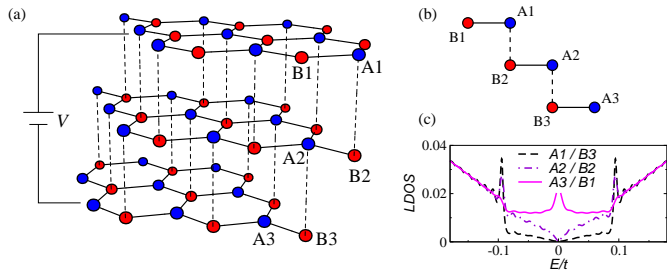


Figure 2: (color online) (a) Trilayer lattice structure. (b) Scheme indicating in-plane (full line) and inter-layer (dashed line) nearest neighbor hopping between different sublattices. (c) LDOS at the three non-equivalent sites in perfect trilayer.

$$H_{TB} = \sum_{i=1}^3 H_i + \gamma_1 \sum_{\mathbf{R}, \sigma} [a_{1,\sigma}^\dagger(\mathbf{R})b_{2,\sigma}(\mathbf{R}) + a_{2,\sigma}^\dagger(\mathbf{R})b_{3,\sigma}(\mathbf{R}) + \text{h.c.}], \quad (3)$$

with H_i being the SLG Hamiltonian

$$H_i = -t \sum_{\mathbf{R}, \sigma} [a_{i,\sigma}^\dagger(\mathbf{R})b_{i,\sigma}(\mathbf{R}) + a_{i,\sigma}^\dagger(\mathbf{R})b_{i,\sigma}(\mathbf{R} - \mathbf{a}_1) + a_{i,\sigma}^\dagger(\mathbf{R})b_{i,\sigma}(\mathbf{R} - \mathbf{a}_2) + \text{h.c.}], \quad (4)$$

where $a_{i,\sigma}(\mathbf{R})$ [$b_{i,\sigma}(\mathbf{R})$] is the annihilation operator for electrons at position \mathbf{R} in sublattice A_i (B_i), $i = 1, 2, 3$, and spin σ , and \mathbf{a}_1 and \mathbf{a}_2 are the primitive vectors of the underlying Bravais lattice. If a perpendicular electric field is applied [11], the following potential energy should be added to Eq. (3),

$$H_V = \frac{V}{2} \sum_{\mathbf{R}, \sigma} [n_{1,\sigma}(\mathbf{R}) - n_{3,\sigma}(\mathbf{R})], \quad (5)$$

with $n_{i,\sigma} = a_{i,\sigma}^\dagger(\mathbf{R})a_{i,\sigma}(\mathbf{R}) + b_{i,\sigma}^\dagger(\mathbf{R})b_{i,\sigma}(\mathbf{R})$. We use the same values for in-plane and inter-layer hopping as for AB stacked multilayer graphene [15], which, as we have seen above, imply $\gamma_1/t \sim 0.1 \ll 1$. Extra hopping terms, as long as they preserve the bipartite nature of the lattice, may introduce quantitative changes but not qualitative [23, 22, 28]. Hopping terms that break the bipartite character of the lattice may be treated perturbatively afterwards [18].

The main feature of the ABC compound that makes it different from its Bernal ABA counterpart is the lack of mirror symmetry with respect to the middle layer. As discussed in [29, 30] this type of stacking allows the derivation of a low energy effective hamiltonian which involves only the unlinked atoms (A_1, B_3) given by

$$\mathcal{H}^{eff} = -\frac{v_F^3}{\gamma_1^2} \begin{pmatrix} 0 & k^{*3} \\ k^3 & 0 \end{pmatrix}, \quad (6)$$

where $k = k_x + ik_y$ and $v_F = 3ta/2$, with a the C–C distance. It also guarantees the topological stability of the low-energy chiral effective Hamiltonian and makes its behavior similar to the AB bilayer discussed previously [30]. As it happens in the bilayer case, a gap can be induced in the ABC system by an external gate.

Vacancies are modelled as missing sites in Eq. (3). There are three non-equivalent vacancy sites. As can be inferred from the lattice sketch shown in Fig. 2(b), these sites correspond to a vacancy occurring in sublattice $A1/B3$, $A2/B2$, and $A3/B1$. The LDOS at these three lattice sites is shown in Fig. 2(c) for the perfect lattice (no vacancy present). Despite the oscillatory behaviour due to finite size effects, distinct thermodynamic limit features can be seen [29]. The low energy physics is determined by sublattices $A3/B1$, and at $E = 0$ a Van-Hove singularity develops due to the cubic spectrum $E \sim k^3$. Sublattices $A1/B3$ and $A2/B2$ have a vanishing contribution to the density of states at low energy. Due to interlayer hybridization their contribution is appreciable only for $|E| > \gamma_1$.

3.2. New midgap state: Analytical considerations

From what is known for the single layer and for bernal stacked multilayer graphene we may immediately infer the following.

1. For a vacancy at any of the two possible places in the middle layer of the ABC TLG the zero energy mode is of the new bilayer type: quasi-localised in the middle layer, and delocalised in the adjacent layer not connected to the vacancy.
2. For a vacancy at any of the outer layers, and residing in the sublattice which is connected to the middle layer, then we simply have the single layer solution: a state quasi-localised around the vacancy.
3. For a vacancy at any of the outer layers, but residing in the sublattice which is not connected to the middle layer we have a new solution with amplitude over the three layers simultaneously.

By extension of the bilayer case we expect the new solution to have a quasi-localised component in the layer with the vacancy and a delocalised one in the middle layer. This is nothing but the new bilayer solution for these two components. The correct behaviour of the third component may be determined by the matching procedure used previously [23, 22]. We do not follow such prescription here. Instead, we perform a numerical analysis detailed in the next section. Nevertheless, we may expect this new component to be delocalised as well just based on the continuum, low energy model, Eq. (6) that describes ABC TLG. Far from the vacancy position such component must satisfy $\partial_z^3 \psi(z, \bar{z}) = 0$. As a natural extension of the bilayer case we have the solution $\psi(z, \bar{z}) = z^2 f(\bar{z})$, with $f(\bar{z})$ meromorphic. Assuming, as in the single layer and bilayer cases, that the meromorphic function is the usual $f(\bar{z}) = 1/\bar{z}$, the new component is manifestly delocalised.

3.3. Numerical analysis

As mentioned before, vacancies are introduced in the TLG lattice by elimination of atom sites. In our approach we use a simple tight binding Hamiltonian and do not include any reconstruction in the remaining structure. We have analysed the changes induced in the LDOS for sites around each vacancy for the three different types described. The LDOS is computed by the recursive Green's function method in clusters with

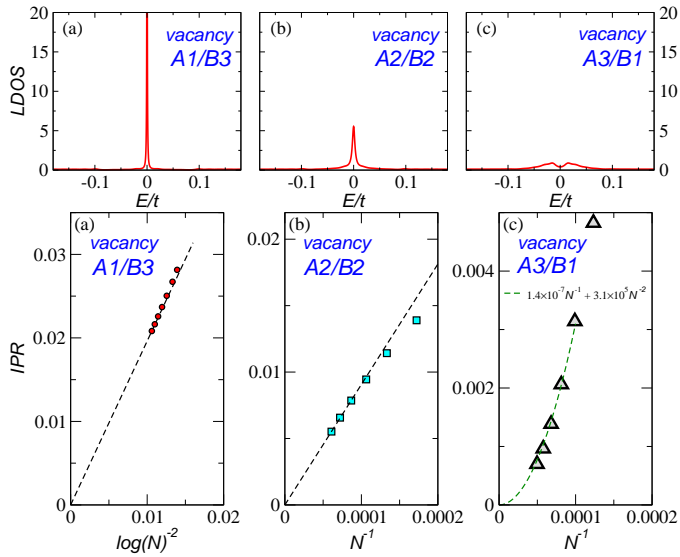


Figure 3: (color online) Upper: LDOS for a vacancy at sublattice (a) A1/B3, (b) A2/B2, and (c) A3/B1. The LDOS is computed at a lattice site closest to the vacancy. Down: IPR for the zero-energy mode induced by the previous vacancies. In panels (a) and (b) linear guide lines are shown to illustrate the scaling. In panel (c) the line is a fit with linear and quadratic terms.

$N = 3 \times 1200^2$, from which the thermodynamic limit can be inferred.

The localisation character of vacancy-induced modes is studied through finite-size-scaling of the inverse participation ratio (IPR). The later is defined as

$$\mathcal{P}_\nu = \sum_i^N |\varphi_\nu(i)|^4 \quad (7)$$

for the eigenstate ν , where $\varphi_\nu(i)$ is its amplitude at site i . We perform exact diagonalization on small clusters with N up to 3×82^2 sites. The IPR for *extended*, *quasi-localized*, and truly *localized* states scales distinctively with N [31]. While for extended states we have $\mathcal{P}_\nu \sim N^{-1}$, for quasi-localized states the $1/r$ decay implies $\mathcal{P}_\nu \sim \log(N)^{-2}$ (consequence of the definition of the IPR in terms of normalized eigenstates). For localized wavefunctions the significant contribution to \mathcal{P}_ν comes from the sites in which they lie, and a size independent \mathcal{P}_ν shows up.

3.3.1. Gapless case

The LDOS and corresponding IPR are shown in Fig. 3 for the three types of vacancy states discussed in this work. The LDOS shown in the upper part is computed at a lattice site closest to the vacancy. We can see a sharp resonant peak for the first type of vacancy in panel 3(a) that corresponds to the state common to the monolayer. The wave function has amplitude only in the layer of the vacancy and is quasi-localised in the opposite sublattice. The $1/r$ decay of the wave function is apparent from the IPR shown in the down part 3(a).

The middle panel 3(b) depicts the results obtained for the vacancy A2/B2. This type of vacancy, also existing in the bilayer AB, is quasi-localised in one layer (where the vacancy

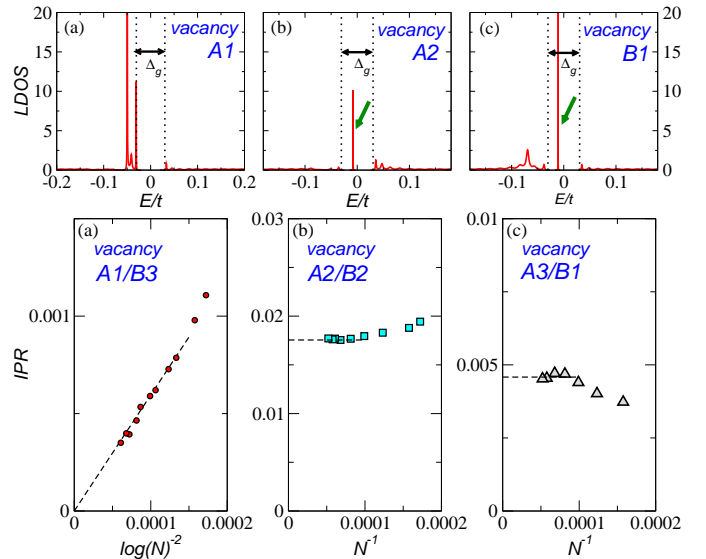


Figure 4: (color online) Upper: LDOS for a vacancy at sublattice (a) A1/B3, (b) A2/B2, and (c) A3/B1 for a finite gap, $V = 0.1t$. The LDOS is computed at a lattice site closest to the vacancy. Localized modes inside the gap are signaled by the arrow. Δ_g . Down: IPR for a vacancy at sublattice (a) A1/B3, (b) A2/B2, and (c) A3/B1 for a finite gap, $V = 0.1t$. As usually done in regions of continuum DOS, the IPR in (a) is an average over states in an energy bin $\Delta E = 0.3t$ around the gap-edge resonance shown in the upper part (a). In (b) and (c) the IPR is for the in-gap mode shown in the upper part. Lines are guides to the eyes.

sits) and delocalised in the adjacent layer where it remains constant when $r \rightarrow \infty$. This behaviour can be seen as a broader feature in the LDOS (upper part 3(b)) that can be attributed to the quasi-localized component in the layer where the vacancy sits (and thus the feature). This interpretation is fully corroborated by the IPR scaling analysis shown in the down part 3(b).

Panel 3(c) shows the behaviour of the new vacancy state found in this work. The absence of a distinct resonance around zero energy is a clear indication that the wave function of this vacancy has amplitude in all three layers. The feature associated with the quasi-localised component in the layer where the vacancy resides is thus weaker than in the other cases, and is buried in the continuum background of band states. The results for the IPR (lower panel) 3(a) confirm the behaviour predicted by the general arguments done in Sec. 3.2. The IPR scales as N^{-1} as corresponds to an extended state, even though finite size effects are quite strong in this case (higher powers of N^{-1} are necessary to fit the data).

3.3.2. Gapped case

The ABC TLG presents, as the AB BLG, the possibility of opening and controlling a gap in the spectrum by applying an external electric field E_z . We have studied the behaviour of the midgap states when a gap opens. We consider a gap induced through a perpendicular electric field $E_z = V/(ed)$, where $d \approx 0.34$ nm is the interlayer distance. Its presence is modelled by adding an on-site energy term: $-V/2$ at layer 1 and $V/2$ at layer 3, as given by Eq. (5).

The results for the gapped case are shown in Fig. 3.3.2. We plot the LDOS (upper panel) and IPR (lower panel) for the three

different types of vacancies.

The first type of vacancy state 3.3.2(a), corresponds to the monolayer type having amplitude only in the layer where the vacancy sits. From the LDOS it can be seen that the quasi-localised state shown in the upper panel of Fig. 3(a), becomes a resonance around $\pm V/2$ in the gaped case. The "monolayer" vacancy 3(a) becomes delocalised at the gap edge. The IPR for this case is an average over the gap-edge resonance shown in the LDOS.

The LDOS for the vacancies of the types 3(b) and 3(c) (upper panel) show that they live inside the gap. We have ascertained this result performing calculations for different gap sizes. Their asymmetric weight over the two layers explains why they appear off zero-energy. The IPR scaling to a constant (lower panel) shows that these vacancies give rise to truly localised states inside the gap. This is the same behaviour encountered for the bilayer case in [22].

4. Conclusions and discussion

We have analysed the various midgap states that arise from the presence of vacancies in multilayer graphene with special emphasis on their degree of localisation. Previous works based on a generalisation of the construction of vacancy states in bilayer AB to multilayer compounds with Bernal (AB) stacking found very different localisation properties for the two different types of vacancies that are present in these compounds. We have completed these works by analysing the rhombohedral ABC trilayer graphene and found yet another new type of vacancy states. Based in tight binding arguments one can show that the new vacancy state survives beyond three layers. In the rhombohedral multilayer the amplitude spreads over all layers, though decaying exponentially as $(\gamma_1/t)^n$ away from the layer where the vacancy sits ($n = 0$). We can also apply continuum arguments. It was shown in [30] that the general rhombohedral stacking including the links $(A_1 - B_2, A_2 - B_3, \dots, A_{N-1} - B_N)$ admits a low energy effective hamiltonian which involves only the unlinked atoms (B_1, A_N) , given by

$$\mathcal{H}^{eff} \sim -\frac{(t/a)^N}{\gamma_1^{N-1}} \begin{pmatrix} 0 & k^{*N} \\ k^N & 0 \end{pmatrix} \quad (8)$$

and hence the new vacancy state found in the ABC trilayer for the B_1-A_3 is directly generalizable to B_1-A_N in the multilayer rhombohedral compounds. This finding exhausts the possibilities for the types of vacancy states in multilayer graphenes in the two more common stacking.

A very interesting open issue is the fate of these states for the twisted multilayers [32, 33] although it is probable that the described features will persist for the vacancies having the same neighbours in the twisted superlattice as the ones described here.

The magnetic behaviour associated to the two types of vacancies of the bilayer system was analysed in [28]. The fully localised midgap states arising from the new vacancy states in the presence of a gap will give rise to fully localised magnetic moments that will play a predominant role in the magnetic behaviour of the samples.

5. Acknowledgments

Support from the Spanish Ministry of Science and Innovation (MICINN) through grants PIB2010BZ-00512 and FIS2011-23713 is acknowledged.

References

- [1] J. B. Oostinga, H. B. Heersche, X. Liu, A. F. Morpurgo, L. M. K. Vander-sypen, Nat. Mater 7 (2008) 151.
- [2] M. F. Craciun, S. Russo, M. Yamamoto, J. B. Oostinga, A. F. Morpurgo, S. Thruha, Nat. Nanotec. 4 (2009) 383.
- [3] T. Khodkov, F. Withers, D. Hudson, M. F. Craciun, S. Russo, Appl. Phys. Lett. 100 (2012) 013114.
- [4] A. A. Avetisyan, B. Partoens, F. M. Peeters, Phys. Rev. B 81 (2010) 115432.
- [5] W. Bao, et al., Nat. Phys. 7 (2011) 948.
- [6] C. H. Lui, Z. Li, Z. Chen, P. V. Klimov, L. E. Brus, T. F. Heinz, Nano Lett. 11 (2011) 164.
- [7] E. McCann, V. I. Fal'ko, Phys. Rev. Lett. 96 (2006) 086805.
- [8] E. V. Castro, K. S. Novoselov, S. V. Morozov, N. M. R. Peres, J. M. B. Lopes dos Santos, J. Nilsson, F. Guinea, A. K. Geim, A. H. Castro Neto, Phys. Rev. Lett. 99 (2007) 216802.
- [9] M. Koshino, E. McCann, Phys. Rev. B 79 (2009) 125443.
- [10] F. Zhang, B. Sahu, H. Min, A. H. MacDonald, Phys. Rev. B 82 (2010) 035409.
- [11] C. H. Lui, Z. Li, E. Cappelluti, T. F. Heinz, Nat. Phys. 7 (2011) 944.
- [12] S. H. Jhang, et al., Phys. Rev. B 84 (2011) 161408(R).
- [13] F. Banhart, J. Kotakoski, A. V. Krasheninnikov, ACS Nano 5 (2010) 26.
- [14] J. C. Meyer, C. O. Girit, M. F. Crommie, A. Zettl, Nature 454 (2008) 319.
- [15] A. H. Castro Neto, F. Guinea, N. M. R. Peres, K. S. Novoselov, A. K. Geim, Rev. Mod. Phys. 81 (2009) 109.
- [16] O. V. Yazyev, Rep. Prog. Phys. 73 (2010) 056501.
- [17] M. P. López-Sancho, F. de Juan, M. A. H. Vozmediano, Phys. Rev. B 79 (2009) 075413.
- [18] E. V. Castro, M. P. López-Sancho, M. A. H. Vozmediano, Phys. Rev. B 84 (2011) 075432.
- [19] R. R. Nair, M. Sepioni, T. I. Ling, O. Lehtinen, J. Keinonen, A. V. Krasheninnikov, T. Thomson, A. K. Geim, I. V. Grigorieva, Nat. Phys. 7 (2012).
- [20] M. Monteverde, C. Ojeda-Aristizabal, R. Weil, K. Bennaceur, M. Ferrier, S. Guéron, C. Glattli, H. Bouchiat, J. N. Fuchs, D. L. Maslov, Phys. Rev. Lett. 104 (2010) 126801.
- [21] M. M. Ugeda, I. Brihuega, F. Guinea, J. M. Gómez-Rodríguez, Phys. Rev. Lett. 104 (2010) 096804.
- [22] E. V. Castro, M. P. López-Sancho, M. A. H. Vozmediano, Phys. Rev. Lett. 104 (2010) 036802.
- [23] V. M. Pereira, F. Guinea, J. M. B. Lopes dos Santos, N. M. R. Peres, A. H. Castro Neto, Phys. Rev. Lett. 96 (2006) 036801.
- [24] L. Zhang, Y. Zhang, J. Camacho, M. Khodas, I. Zaliznyak, Nat. Phys. 7 (2011) 953.
- [25] S. Yuan, R. Roldán, M. I. Katsnelson, Phys. Rev. B 84 (2011) 125455.
- [26] R. van Gelderer, L. Lim, C. Morais-Smith, Phys. Rev. B 84 (2011) 155446.
- [27] A. Kumar, et al., Phys. Rev. Lett. 107 (2011) 126806.
- [28] E. V. Castro, M. P. López-Sancho, M. A. H. Vozmediano, New Journal of Physics 11 (2009) 095017.
- [29] F. Guinea, A. H. Castro Neto, N. M. R. Peres, Phys. Rev. B 73 (2006) 245426.
- [30] J. L. Mañes, F. Guinea, M. A. H. Vozmediano, Phys. Rev. B 75 (2007) 155424.
- [31] V. M. Pereira, J. M. B. Lopes dos Santos, A. H. Castro Neto, Phys. Rev. B 77 (2008) 115109.
- [32] J. M. B. L. dos Santos, N. M. R. Peres, A. H. Castro Neto, Phys. Rev. Lett. 99 (2007) 256802.
- [33] L. Brown, R. Hovden, P. Huang, M. Wojcik, D. A. Muller, J. Park, Nano Lett. (2012).